Optimization of Wavefront Control using a High Resolution Wavefront Sensor

Willie Franceschi
Victor Senior High School
Advisers: Brian Kruschwitz, Adam Kalb

University of Rochester
Laboratory for Laser Energetics
Summer High School Research Program
June 2015

Optimization of Wavefront Control using a High Resolution Wavefront Sensor

Abstract

The use of adaptive optics to correct the laser wavefront is a key component of the Omega EP laser. This correction is based on information provided by a wavefront sensor (WFS). Compared with the 77 resolution elements of the current wavefront control sensor, the high-resolution wavefront sensor (HRWS) contains 19,044 resolution elements (138 by 138), allowing for more accurate wavefront measurements and potentially improved wavefront correction. The incorporation of this sensor required modifications to previous software and writing of new MATLAB code for diagnostic and stability purposes. In order to solve the issue of a changing pupil area, a "global pupil" approach was developed and implemented in the calibration and correction processes. The testing of correction software, including the global pupil approach, was conducted in the deformable mirror (DM) testbed. The HRWS control algorithms were tested on a beamline of the Omega EP laser, and outperformed the existing Wavefront Control System with an 8% decrease in RMS wavefront error and a 5% decrease in focal spot size (80% encircled energy). The correction of two deformable mirrors simultaneously was also attempted, with mixed results.

Introduction

Due to a variety of factors, including aberrations in amplifiers and optics, the laser beam wavefront on the Omega EP laser system is not flat, resulting in poorly focused focal spots upon target. To minimize this effect, the Omega EP laser includes a series of wavefront control loops, or adaptive optics systems, that work to correct the wavefront aberrations (1). A simplified diagram of the wavefront control loop is shown in figure 1, demonstrating the process in which this aberrated wavefront is corrected. An adaptive optics system - in this case a deformable mirror - physically corrects the wavefront. The corrected laser beam continues on to the target (2).

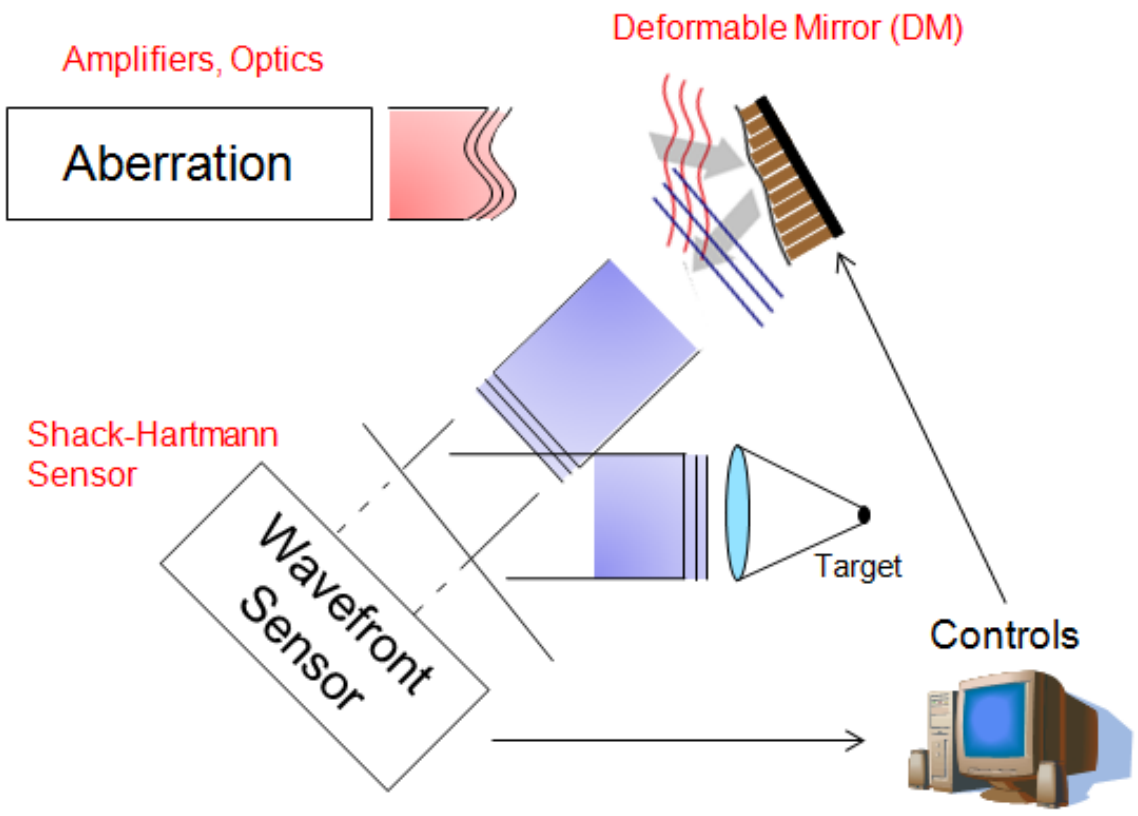

Figure 1: *An adaptive optics system used to correct the uneven wavefront produced by amplifiers and optics. A wavefront sensor measures the corrected wavefront and sends the data to a control system. The control system processes the data and adjusts the deformable mirror, further correcting the wavefront by altering the voltages of the 39 actuators spread out behind the mirror.*

The Omega EP DM has a reflective surface approximately 400 mm by 400 mm square. Actuators assembled in a hexagonal pattern push and pull on the backside of the mirror to create a deformed surface that corrects the uneven wavefront. Voltages are applied to these actuators, and the actuators move accordingly (104 nm per volt). All the actuators have lower and upper voltage limits at 30 and 150 volts respectively. Occasional issues with actuators reaching, and stalling, at upper and lower voltage limits were corrected through MATLAB software discussed later in the paper.

The wavefront sensors used in the Omega EP wavefront control system are Shack-Hartmann sensors (SHS). A SHS is composed of a two-dimensional array of lenses that focuses different parts of a beam of light onto a flat sensor. The sensor measures the offsets of these focused points (centroid locations or offsets) in the horizontal and vertical directions, relative to the centroid locations of a reference, flat wavefront (3). The sensor stores information about the horizontal and vertical offsets of the wavefront that the controls use in correction algorithms. Different wavefront aberrations cause varying centroid offsets.

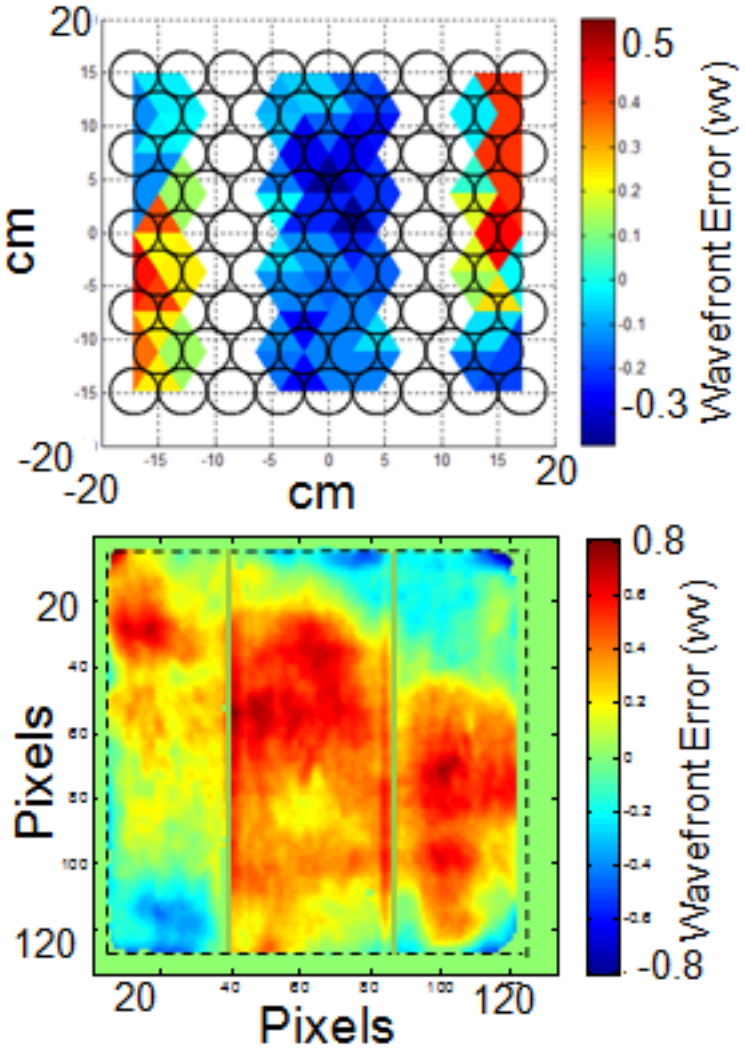

Figure 2: *Wavefront images produced by the current, 77-resolution element sensor (top) and the HRWS (bottom). The superior wavefront imaging quality and resistance to tilted diffraction grating gaps (2 vertical lines missing light on both images) are shown in the bottom image.*

Figure 2 shows a comparison of wavefront images produced by the current WFS and the HRWS. Aside from the clear advantages in the definition of the image of the wavefront, the HRWS image is less affected by the loss of light due to the tilted diffraction gratings (each grating is split into three "tiles"). The two vertical columns lacking light are caused by the gaps in the tiled diffraction grating assemblies in the lower compressor (the compartment at the latter end of the beam line in which the nanosecond input pulse is shortened to a picosecond output pulse) of the OMEGA EP laser. The current wavefront sensor shows a wavefront that is highly affected by the loss of light in those vertical areas, as seen by the missing light in a significant portion of the resolution elements. The diffraction grating gaps, however, do not affect the image of the HRWS wavefront nearly as badly. The loss of two vertical columns of resolution elements affects the wavefront image less when there are 138 columns of resolution elements.

Given a measured wavefront image, the 39 actuator voltages that need to be applied to the DM actuators to correct the wavefront are determined using a control matrix (C). The control matrix is formed in the calibration process. In this process, each actuator is pushed out a known amount and the response of the wavefront is stored into a response matrix (R) with 39 columns (39 actuators) and 38,088 rows (19,044 resolution elements with x and y displacements) when the HRWS is being used. The response matrix has one column filled each time an actuator is pushed out. After the response matrix is filled, it is pseudo-inverted to create a control matrix with 39 rows and 38,088 columns. Pseudo-inversion refers to the algorithm (described in ref. 4) whereby the control matrix is determined from the response matrix. The number of rows in the response matrix and the subsequent number of columns of the control matrix are dependent on the number of resolution elements in the wavefront sensor (4).

Matrix multiplication is used to determine the actuator voltages necessary for wavefront correction, as shown in figure 3. The control matrix is multiplied by an array (S) of centroid offsets. After a scalar multiplication by the "gain" which is a scalar value that enhances the stability of the correction process, a 39-element array of necessary voltage changes is produced.

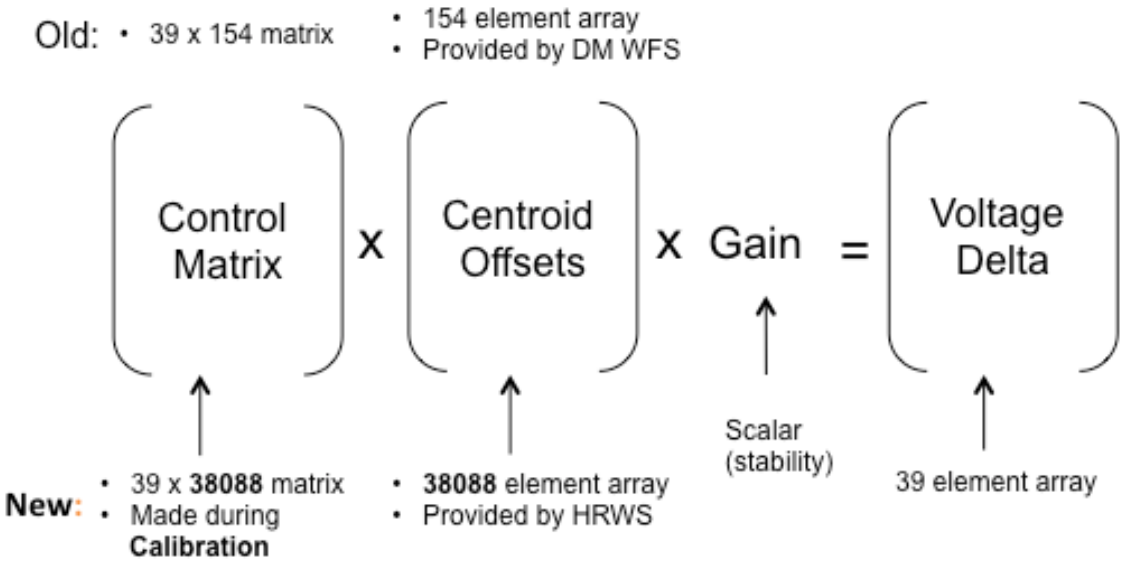

C = control matrix S = centroid offsets g = gain R = response matrix ΔV = voltage delta

$$C \cdot S \cdot g = \Delta V$$

Figure 3: *The matrix multiplication used in wavefront correction to determine the voltage changes ΔV to be applied to the actuators from the known matrices C and S. The dimensions labeled "old" correspond to the dimensions of the matrices when the 77-resolution element sensor was used.*

This project involved the writing of computer code using MATLAB to incorporate the HRWS into the wavefront control system. Various diagnostic and stability deficiencies required new code, as well as alterations to existing code. The new control system was tested and debugged on the deformable mirror testbed. Experiments on the Omega EP laser system were then conducted and showed improved wavefront correction.

MATLAB code

The following scripts and functions were written in this work: *fizeaudataanalysis*, *plotDMwavefront*, *tiltmonitoring*, *continuouswave*, *midTravel*, and *omegaepcontrol*. The first four functions and scripts have diagnostic purposes. The last two have stability purposes.

fizeaudataanalysis is a script that allows the user to obtain images and wavefront values from the Fizeau interferometer. *plotDMwavefront* is a function that uses the actuator voltages to calculate the wavefront of the deformable mirror. *tiltmonitoring* is a function that calculates the horizontal and vertical tilt of the deformable mirror based on the actuator voltages. *continuouswave* is a script with multiple parts that can display single or continuous images of the raw intensity or wavefront information obtained from the HRWS camera. These four functions and scripts were written for diagnostic purposes during the debugging of the control system. *midTravel* is a function that prevents the actuator voltages on the deformable mirror from reaching their upper or lower limits. This function increases or decreases all the actuator voltages by the same amount to prevent any gradual upward or downward shift in voltages after multiple correction iterations. *omegaepcontrol* is a script with multiple parts allowing user-specified correction of specific deformable mirrors on a beam line in the OMEGA EP laser. For example, there are two deformable mirrors in the first beamline of the OMEGA EP laser. *omegaepcontrol* is a script in which the user can run correction algorithms on a specific deformable mirror alone or on both DMs at the same time by running different sections of code, and record the RMS wavefront and gradient values of the corrected wavefront after each correction iteration.

The following alterations were made: controlling both deformable mirrors simultaneously and incorporating a “global pupil” algorithm into the calibration process. The global pupil algorithm is used to ensure that resolution elements typically near the edge of the beam that do not consistently record data throughout the calibration process are not used in the calculation of the control matrix. These alterations built upon previous code authored by Adam Kalb for the current wavefront system. The simultaneous controlling of both deformable mirrors in a beam line required various alterations to previous calibration, corrections, and voltage setting code. The specifics of these

alterations and their ultimate goal will be discussed below. Incorporating a global pupil was a solution to an issue with the HRWS of a changing pupil size.

Deformable Mirror Testbed and Troubleshooting

Before any new code could be tested, the DM testbed was set up and debugged. A top view of the DM testbed can be seen in figure 4. Much of the optics, specifically around the flip-up mirror and cameras, was set up and aligned. The HRWS was also installed and its optimal light intensity was found.

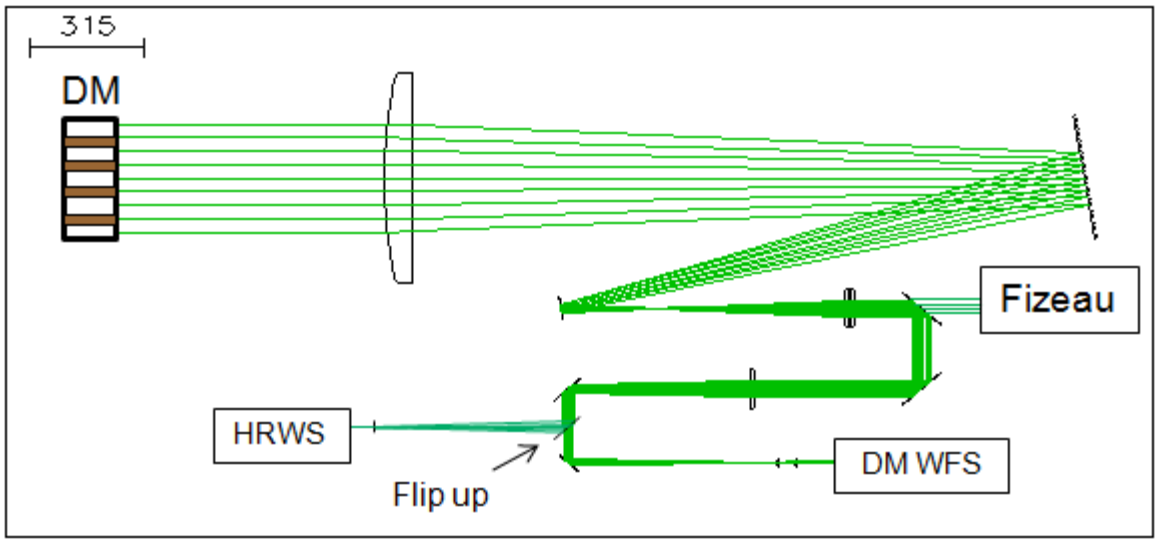

Figure 4: *The DM testbed setup. The light beam originates at the Fizeau interferometer. This beam continues on to a deformable mirror, and is then directed back through a series of mirrors and lenses to a wavefront sensor. Either the current wavefront sensor DM WFS or the HRWS receives light based on whether the flip-up mirror is up or down.*

A few lingering hardware problems made early testing of code difficult. The HRWS had some inaccuracies in imaging that complicated the calibration process. It is important to note that these inaccuracies did not impact the code testing. The minor inaccuracies were present during the whole process so all of the reference and corrected wavefront measurements had to deal with them. As testing progressed, these HRWS camera issues were mitigated.

The other, more prominent, hardware difficulty was a malfunctioning of the DM actuator electronics. As testing of code progressed, inconsistencies with wavefront correction persisted. For example, a correction iteration would adversely affect the quality of the wavefront instead of improving it. During the debugging process, it was discovered that some of the actuators were responding abnormally slowly. A longer pause was inserted into the calibration and correction processes with little improvement. Eventually, multiple failed resistors were discovered in the driver electronics. After replacement of these resistors in the drive board, code testing became much more consistent.

"Global Pupil Algorithm"

A "global pupil" algorithm was implemented to counter the issue of a changing pupil. A changing pupil means that light is present in a resolution element in the HRWS during the calibration of one actuator but not present during the calibration step of another actuator. This occurs primarily at the edges. This leads to inconsistent response matrix values corresponding to the inconsistent centroid locations. The control algorithms cannot accurately control the actuators. This issue with inconsistencies in the presence of light was not present with the current 77-resolution-element wavefront sensor. The current wavefront sensor has resolution elements of much greater size, decreasing the chance of inconsistent light fluctuations within each resolution element. Slight vibrations in the OMEGA EP laser would not affect the presence of light nearly as much as it would with the 19,044-resolution element HRWS. With the much smaller resolution elements in the HRWS, these slight vibrations cause light to shift in and out of resolution elements. This problem is illustrated in figure 5. The detailed view of the edge of the pupil shows how slight vibrations can easily alter the presence of light in certain resolution elements. A pupil is defined as a 138 by 138 element matrix, corresponding to resolution elements in the HRWS, with ones where there is light and zeros where there is no light.

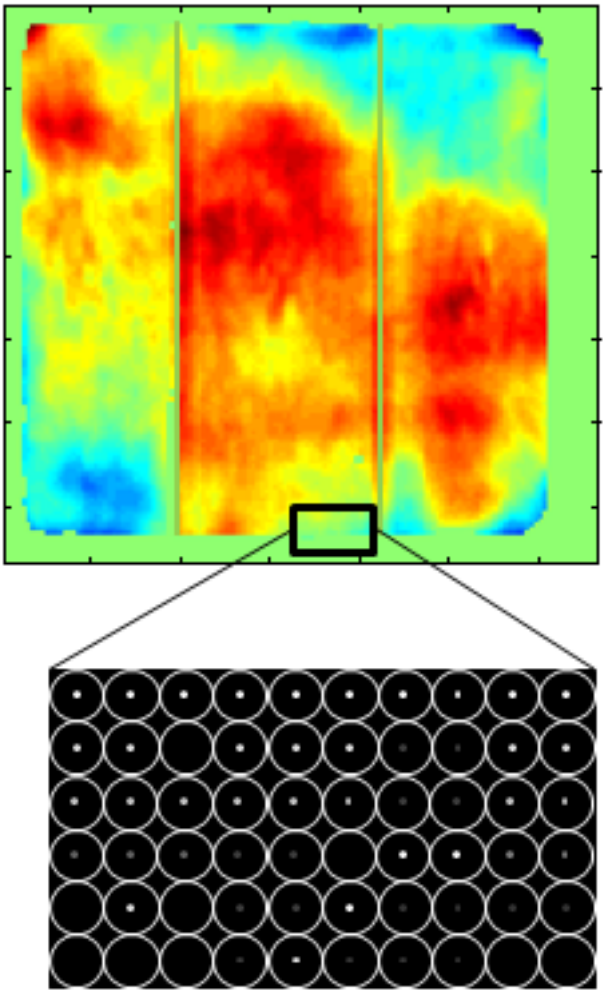

Figure 5: *A detailed diagram of the presence of light in resolution elements at the edge of the pupil (bottom). The wavefront image (top) is the same as in figure 2. The bottom diagram shows the lack of a definitive edge when a beam of light is captured by the HRWS. This allows slight vibrations to affect the distribution of light among these resolution elements.*

With the global pupil approach, only centroid locations with light present during the whole process are used in the correction process. This means that only offsets in these centroid locations would be corrected. This avoids any confusion between actuators concerning which centroids to correct. This approach was implemented through alterations to the calibration code. At the beginning of the calibration process, a pupil is obtained from the HRWS camera. Whenever a new wavefront image is obtained by the HRWS camera, a pupil is extracted and element-wise multiplied by the previous pupil. This new pupil is stored as an external variable that constantly gets smaller (some places with ones get replaced with zeros) as the calibration continues. A new pupil is obtained by the camera at least once every calibration step. After all the actuators have been calibrated and a response matrix has been formed, the new pupil, now known as the

global pupil, is made into a 38,088 element array. This global pupil matrix is element-wise multiplied by each column of the response matrix to remove any rows that correspond to inconsistent centroid locations. Any elements with a zero in the global pupil (centroid locations in which light was not present during the whole process) make the corresponding elements in the response matrix a zero. The response matrix is pseudo-inverted to create a 39 by 38,088 element control matrix. At this point, the DM actuators are able to correct consistent centroid locations.

It is important to note that filling a row of the response matrix with zeros before pseudo-inverting it (as done with the 38,088 by 39 response matrix to transform it into a 39 by 38,088 control matrix) does not adversely affect the resulting control matrix. With the many resolution elements without light in the HRWS, confirming resistance of the pseudo-inverting process to zeros was vital. To test this, a 4x4 matrix of random numbers was created. This was inversed, then multipled by a 4x1 matrix of random numbers. Next, a 12x4 matrix was created by inserting 2 rows of zeros after each row of the original 4x4 matrix. The 12x4 matrix was then pseudo-inverted and multiplied by a 12x1 matrix, which was created by inserting two rows of zeros after each row of the previous 4x1 matrix. The products from the first and second inversion tests were identical. This validated the pseudo-inverting process with the matrix multiplication using a HRWS.

In order to test the effectiveness of the global pupil approach, wavefront corrections were conducted with a control matrix generated using the global pupil in the calibration process and compared to wavefront corrections using a control matrix without the global pupil in the calibration algorithm. For consistency, the starting wavefront before correction was a reference flat wavefront. A flat mirror was set up in the place of the deformable mirror in the DM testbed and the wavefront was recorded in the HRWS, current wavefront sensor, and Fizeau interferometer software. After the reference wavefront was recorded, the deformable mirror replaced the flat mirror. Before a wavefront correction was tested, a known aberration was applied to the wavefront by manually changing the voltages of the DM actuators. Before each wavefront correction, 85 volts were applied to each DM actuator, producing a consistently biased wavefront for each correction test. The deformable mirror was then calibrated, producing a control matrix. Two calibrations were performed, one with the global pupil and one without.

Each control matrix was saved, and later loaded when wavefront correction tests were conducted.

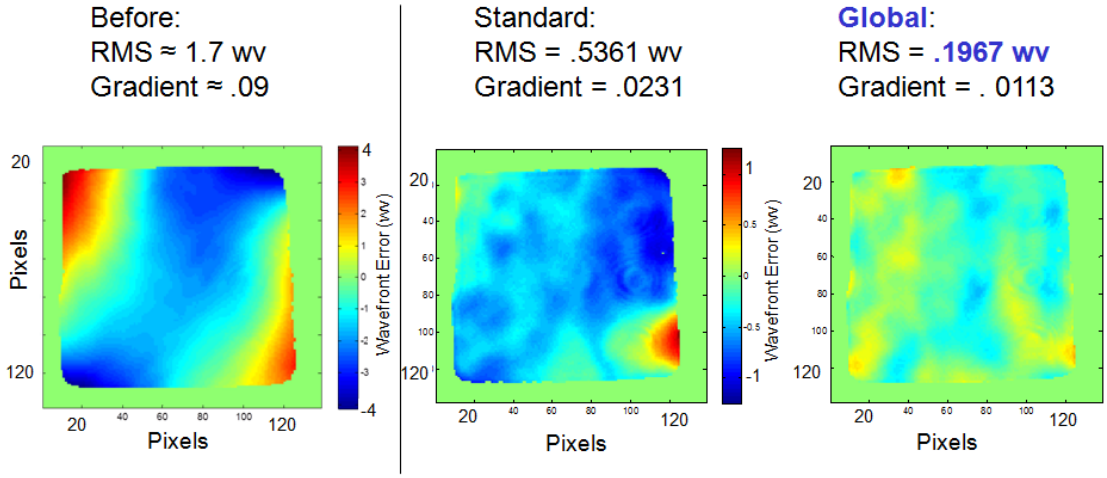

Figure 6: *The comparison between wavefront correction with and without the global pupil approach after 100 iterations. This test was conducted in the DM testbed. The lower RMS wavefront and gradient values attained with wavefront correction using the global pupil can be seen. The colorbar is four times greater in range in the biased wavefront image (on the left) compared to the two corrected wavefront images. The two corrected wavefronts use the same colorbar.*

The results of the global pupil tests can be seen in figure 6. The wavefront corrections using a control matrix generated without a global pupil, called a "standard" pupil in the figure, attained an RMS wavefront value of 0.5361 waves (wv) and a gradient (overall tilt) of 0.0231. Wavefront correction using the control matrix generated with the global pupil attained an RMS wavefront value of 0.1967 wv and a gradient of 0.0113. The aberrated wavefront applied before both corrections is shown on the left. The advantages of the global pupil are also seen in the wavefront images. The image after correction with the standard pupil control matrix has a red dot in the corner, which shows a DM actuator that did not correct properly. This was a common characteristic when correcting a wavefront with the standard pupil. When correcting the wavefront using the global pupil approach, however, the correction algorithm did not produce incorrect voltage changes, allowing the DM actuators to create a more uniform, flatter wavefront.

With 19,044 resolution elements in the HRWS, there was also some concern that errors accumulated during the matrix multiplication of the wavefront correction process could, after many iterations, cause the correction process to become unstable. This has occurred with the current system on a laser beamline where multiple corrections were consecutively applied throughout the day. 100 iterations of wavefront correction were conducted for the global pupil and standard pupil control matrices. The graph in figure 7 shows the stability of wavefront correction using the HRWS. The superiority of the global pupil control matrix can be seen on the graph as well. The RMS wavefront values attained through correction using the global pupil control matrix are clearly lower compared to wavefront correction using the standard pupil control matrix. Also, the global pupil correction algorithm converges to its final wavefront correction within 10 iterations.

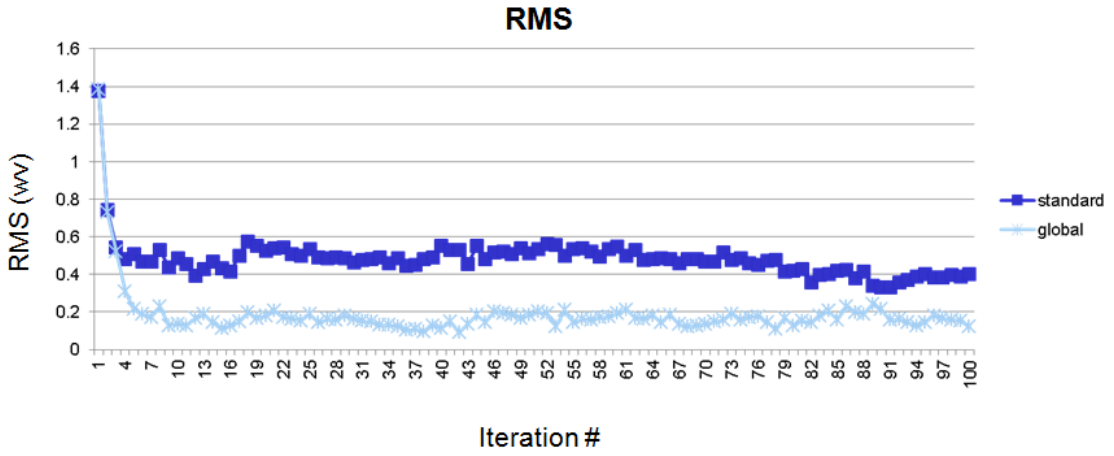

Figure 7: *RMS wavefront error plotted against wavefront correction iteration number for standard and global pupil algorithms. 100 iterations of wavefront correction using the HRWS correction algorithms were conducted in the DM testbed. The correction algorithm without the global pupil (standard pupil) and the algorithm with the global pupil started with an initial aberration in the wavefront. Both correction algorithms approached and hovered around a certain RMS wavefront value, confirming that wavefront correction using the HRWS is stable.*

Once wavefront correction using a HRWS was optimized (using the global pupil method), the optimized MATLAB software was tested on the OMEGA EP laser and its wavefront correction capabilities were compared to those obtained with the current 77 resolution element wavefront sensor using the current wavefront sensor correction software. The results can be seen in figure 8. Using the current 77-element wavefront sensor, the correction algorithm attained a wavefront with an RMS wavefront value of 0.27 wv and an R80 focal spot radius (radius of focused laser beam where 80% of energy is encircled) of 19.0 micrometers. Wavefront correction using the HRWS attained a RMS wavefront value of 0.25 wv and an R80 radius of 18.2 micrometers. Using the HRWS for wavefront correction decreased the RMS wavefront and R80 focal spot values by approximately 8% and 5% respectively. Ideally, this increases the average on-target intensity by approximately 10%. More tests are required to increase confidence in these findings.

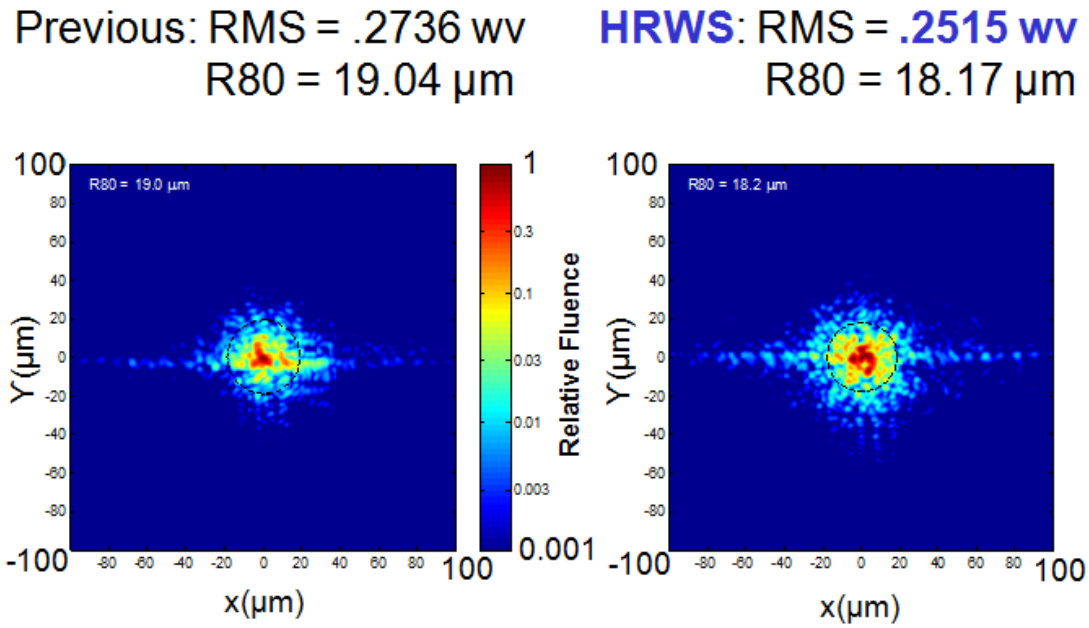

Figure 8: *Focal Spot on Omega EP using (left) wavefront correction with the current, 77-resolution element sensor and (right) wavefront correction with the HRWS.*

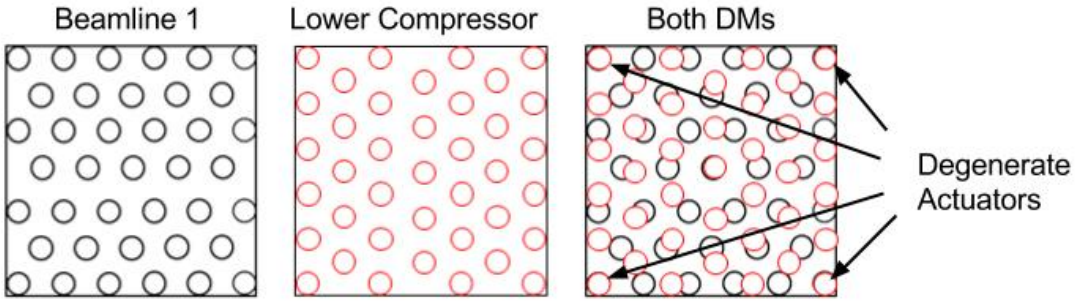

Figure 9: *The arrangement of actuators for each DM. The overlapped arrangement of actuators - when both DMs are corrected simultaneously - is shown on the right. The primary degenerate actuators are labeled.*

Simultaneous Correction of Two Deformable Mirrors

On the two short-pulse beamlines of the OMEGA EP laser, two deformable mirrors are configured in the laser path for each beam. One of these deformable mirrors is located in the amplifier line, and the other is in the compressor. Currently, each deformable mirror is corrected separately. A possible way to improve wavefront correction is to correct both deformable mirrors simultaneously. This means that one correction algorithm would correct both DMs using a control matrix with twice as many rows (78 combined actuators). The reason that simultaneous correction can improve wavefront correction is that the two DMs are oriented at 90° to each other as shown in figure 9. This causes more actuators to physically cover the wavefront. If the 78 actuators correct at the same time, there are more actuators per surface area, theoretically increasing the quality of wavefront correction. After a few correction iterations, the results are shown in figure 10. As was expected, simultaneous correction slightly improved wavefront correction compared to the previous method of separate deformable mirror correction.

After more than a few iterations, the simultaneous correction of both deformable mirrors caused problems due to the spacing of the two mirrors. The first deformable mirror began to apply a large wavefront error that was being corrected by the second

mirror, until the wavefront slope became too large to pass through the beamline. Starting at the corners and edges, parts of the beam were lost due to clipping by pinholes in the

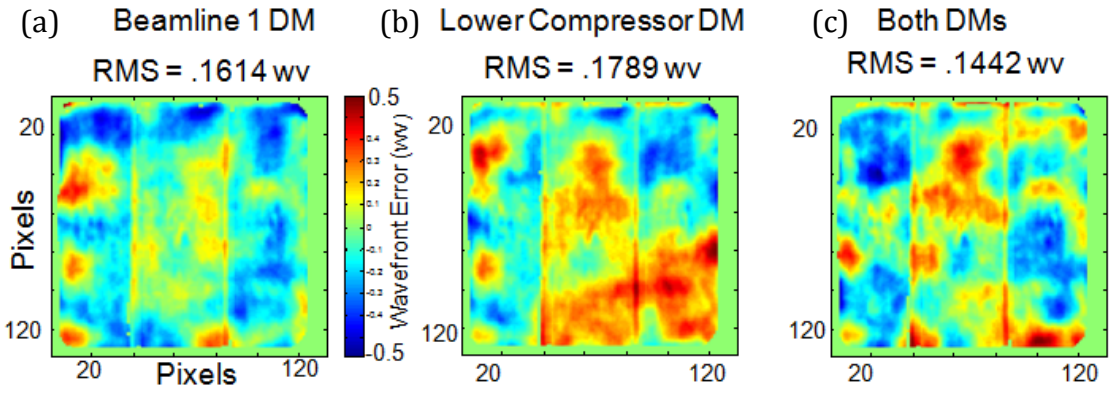

Figure 10: *Comparison of wavefronts obtained by correcting just the beamline 1 DM (a), the Lower Compressor DM (b), and both DMs simultaneously (c). Using the omegaepcorrect script, the deformable mirror in beamline number one of the OMEGA EP laser system underwent 5 correction iterations, and then the lower compressor deformable mirror underwent 5 correction iterations, and finally both deformable mirrors underwent 3 simultaneous correction iterations.*

laser beamline. Upon closer investigation of the actuator diagrams in figure 9, some actuators (corners and middle actuator) overlap; i.e. the actuators are "degenerate" and act on the wavefront identically. The result is one actuator pushing out while the corresponding actuator on the other deformable mirror pulls in. The HRWS at the end of the laser path does not realize this until the wavefront tilt from the first mirror's actuators causes the wavefront to be lost in the beamline. As significant portions of the centroid locations are lost, further correction iterations increasingly degrade the quality of the beam.

After unsuccessful attempts at containing actuator voltage values within a certain range, a more specific attempt was made. The primary dysfunctional areas of degradation, the corners, would be fixed by removing the four corner actuators of the beamline number one deformable mirror from the calibration and correction steps. This would mean that only the lower compressor deformable mirror would correct the corners of the

wavefront, avoiding the issues with overlapping corner actuators. The columns in the response matrix corresponding to the four corner actuators were set to zero. When the resulting control matrix was used in wavefront correction, the four corner actuators of the beamline number one deformable mirror remained stationary. Unfortunately, this provided little benefit to the stability of the simultaneous wavefront correction. Instead of three or four iterations, it now took five or six correction iterations before the wavefront began to degrade. The issue at the corners was resolved, but the actuators by the edges also began to experience similar issues of antagonistic displacement with their corresponding actuators. Although these actuators did not overlap, it is likely that nearly overlapping actuators experienced similar issues as the corner actuators.

It is important to note that while the center actuators overlapped between both deformable mirrors, the center of the wavefront did not degrade. This is most likely due to the abundance of information in centroid locations surrounding the center actuators - unlike the corner actuators where fewer surrounding resolution elements contain light - that would be greatly affected by the inaccurate correction caused by detrimental information provided to the center actuator. Also, nearby actuators influence the wavefront differently on each deformable mirror, meaning that the center actuators were not totally "degenerate". Simultaneous correction of both deformable mirrors is a potentially beneficial process, but it requires further investigation to solve the significant issues with antagonistic actuator voltage wandering.

Conclusion

Wavefront correction on the OMEGA EP laser system has been improved by the incorporation of the HRWS and optimization of the correction algorithms, leading to a decrease in the RMS wavefront of the laser beam and the R80 radius by ~8% and ~5%, respectively. This corresponds to an increase in the on-target average intensity by ~10%.

Acknowledgements

I would like to thank Dr. Craxton for granting me the opportunity to take part in the 2014 High School Summer Research Program. Furthermore, I would like to thank my advisors, Dr. Brian Kruschwitz and Adam Kalb, as well as Kyle Gibney for providing tremendous amounts of knowledge, resources and support during the program.

References

1. B. Kruschwitz, "Wavefront Control System for Omega EP," 9 Mar. 2007. *Microsoft Powerpoint* file.

2. S. S. Olivier, "Wavefront Correction Technologies," Summer School for Adaptive Optics. 11 Aug. 2004. Reading. http://cfao.ucolick.org/aosummer/archive/aosummer2004/lectures.php

3. B.C. Platt and R. Shack, "History and Principles of Shack-Hartmann Wavefront Sensing," *J. Refr. Surgery* **17**, S573 - S577 (2001)

4. R. Zacharias, E. Bliss, S. Winters, R. Sacks, M. Feldman, A. Grey, J. Koch, C. Stolz, J. Toeppen, L. Van Atta, and B. Woods, "Wavefront Control of High-Power Laser Beams in the National Ignition Facility (NIF)," in *Advanced High-Power Lasers*, ed. M. Osinski, H.T. Powell, K. Toyoda, Proc. SPIE vol. 3889, 332 - 343 (2000)